

論文 著書情報
Article Book Information

Title	Eccentric Crank Rover - A Novel Crank Wheel Mechanism with Eccentric Wheels
Author	Hirota Komura, Gen Endo, Koichi Suzumori
Journal/Book name	Proceedings of 2016 IEEE/RSJ International Conference on Intelligent Robots and Systems - Vol. 1 - No. 1 - pp. 1048-1053
Issue date	2016-10
DOI	http://dx.doi.org/10.1109/ROSD.2016.7759178
URL	http://www.ieee.org/index.html
Copyright	©2016 IEEE. Personal use of this material is permitted. Permission from IEEE must be obtained for all other users, including reprinting, republishing this material for advertising or promotional purposes, creating new collective works for resale or redistribution to servers or lists, or reuse of any copyrighted components of this work in other works.
Note	このファイルは著者（最終）版です。 This file is author's final version.

Eccentric Crank Rover: A Novel Crank Wheel Mechanism with Eccentric Wheels

Hiroataka Komura¹, Gen Endo¹ and Koichi Suzumori¹

Abstract—The crank wheel mechanism, consisting of a wheel mechanism and parallel links connected to each wheel, achieved high mobility and efficiency because it has both wheels and legs in a simple structure. However, each prior model of crank wheel mechanism has had shortcomings such as mass oscillation or fragile structure. In this paper, we propose a novel crank wheel mechanism, the "Eccentric Crank Rover"(ECR), which is an enhanced crank wheel mechanism with eccentric wheels. The eccentric wheels increase the under-body clearance, and change the body trajectory from straight to trochoid curve, which has the same shape as the crank legs but opposite phase trajectory. Thus, the body itself acts as a "second" crank leg. We experimentally confirmed higher step climbability, larger clearance, and lower cost of transport than other models such as normal wheel model, eccentric wheel model, and crank wheel model without eccentric wheel.

I. INTRODUCTION

In general, wheel type transfer mechanisms have high energy efficiency and simplicity, but lack sufficient mobility on rough terrain like uneven or soft ground. In contrast, continuous track mechanism has high mobility in rough terrain because of its low grounding pressure and large driving area, and this mechanism is used in many mobile robots[1], [2]. However, track-type mechanisms have complex and heavy structures because they comprise many parts such as belts, sprockets, and idlers. This complex structure results in lower energy efficiency than conventional wheeled systems. In addition, the gaps in the belt and sprockets tend to roll up small objects.

Multi-DOF mechanisms, such as legged type or snake type[3], [4], are also applicable for traversing through rough terrain; however, the numerous DOFs render the structure fragile and reduce the energy efficiency.

Further, there are several enhanced wheel mechanisms applicable for rough terrain[5], [6]. However, the energy efficiency of most of them is lower than that of conventional wheel mechanisms because of their oscillations and complex structure.

In contrast, RHex[7] provides high mobility on rough terrain, although its structure is quite simple. The best cost of transport (specific resistance)[8] of RHex and enhanced models of RHex were in the range of 0.5-0.9, including hotel load. These values make RHex a good choice for use as a rough terrain vehicle.

¹H. Komura, G Endo and K Suzumori are with the Department of Mechanical and Aerospace Engineering, Tokyo Institute of Technology, 2-12-1 Ookayama, Meguroku, Tokyo, 152-8552, Japan, komura.h.aa at m.titech.ac.jp, gendo at mes.titech.ac.jp, suzumori at mes.titech.ac.jp

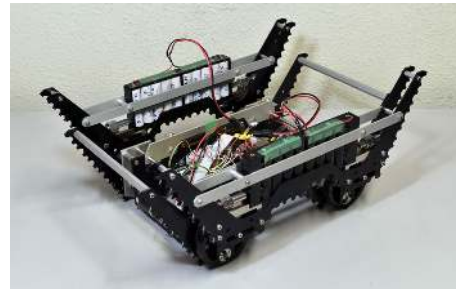


Fig. 1. "Eccentric Crank Rover"

Crank wheel mechanism[9] is another method to achieve good mobility in rough terrain, energy efficiency, and simplicity of mechanism. This mechanism has wheels and parallel links called "crank legs" which are connected to the wheels. On a flat surface, this mechanism uses only the wheels to move. Therefore, this mechanism has the possibility to achieve higher energy efficiency than RHex series, since the cost of transport of cars are quite low (0.05 to 1)[8]. On rough terrain, the crank legs are responsible for the driving area, thereby decreasing its ground pressure and increasing the driving area. Further, grousers in the crank legs affix themselves to the edge of obstacles, thereby enabling the vehicle to navigate over obstacles.

In this research, we propose a novel crank wheel mechanism, "Eccentric Crank Rover"(Fig.1), which is equipped with eccentric wheels, and demonstrate the advantages of this mechanism using physics simulations and experiments.

The features and shortcomings of prior crank wheel models are described in Section II. In Section III, the concept of ECR mechanism is explained. Section IV describes, in detail, design of a hardware prototype of the ECR vehicle. Section V describes the results of the comparative experiments of ECR. Finally, the conclusions of the study are presented at the end of the manuscript.

II. PROBLEMS OF PRIOR MODELS

A. Simple Crank Wheel

Fig.2 illustrates a simple crank wheel mechanism. This mechanism utilizes 4 wheels, similar to that in a conventional wheel mechanism, the difference being that the crank legs are attached to the both sides of the wheels. Each crank leg is connected to the wheel by passive revolution joints in eccentric position. Thus, the body, one pair of front and rear wheels, and one crank leg comprise a parallel link, and the crank legs and the body are kept in a parallel position.

On flat surfaces, the crank wheel mechanism only uses the wheels for mobility. While running on flat surfaces, the

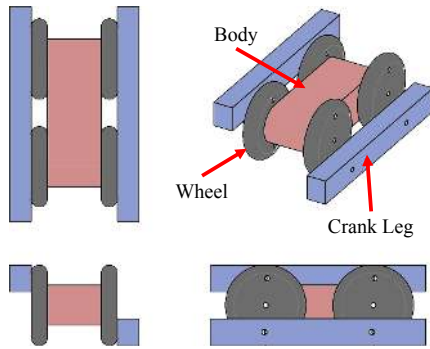


Fig. 2. The simple structure of crank wheel mechanism having 1 pair of crank legs. The crank legs, the body, and the wheels are indicated in blue, red, and gray, respectively.

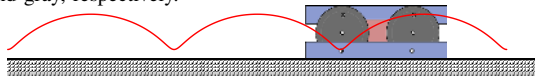


Fig. 3. Trochoidal curve of the crank leg trajectory. This trajectory is similar to that of a foot, when walking.

body maintains its height and posture. In contrast, the crank legs follow a trochoidal trajectory during vehicle motion, as shown in Fig.3. This motion allows the crank legs to act as legs, which push down obstacles and push up the body of the vehicle. Hence, the crank leg mechanism has high mobility, even when navigating through rough terrain.

In terms of energy efficiency, this trochoidal motion generates an oscillation of necessary torque of the wheel as the crank legs move up and down. Thus, in this simple model, the energy efficiency become less than that of a conventional wheel mechanism, depending on the weight of crank legs.

This simple model can realize higher mobility on rough terrain as compared to a conventional wheel model. However, this model does not address the problem faced by vehicles using conventional wheel mechanism; such a wide body with low ground clearance is susceptible to being rendered immobile by protrusions like tree stumps. In other words, the clearance height under the body is insufficient.

B. Prior "Crank-Wheel"

Fig.4 shows prior "Crank-Wheel", and Fig.5 shows the schematic illustration of the Crank-Wheel. This robot has 2 pairs of crank legs. An inverse U-shaped body is incorporated in order to avoid interfering with the inside pair of crank legs. This inverse U-shape is also effective for preventing the vehicle from getting stuck on protrusions like tree stumps. In order to maintain the static balance of the vehicle, the crank legs are attached to the wheels in the opposite phase. Therefore, if the friction in the revolution joints between wheels and crank legs is neglected, the energy required by the vehicle to run on flat surfaces is identical to that of a wheeled vehicle without crank legs.

One of the problems of the Crank-Wheel is the complicated and fragile structure of inverted U-shaped body. The body stiffness is weaker than that of the simple model. In addition, this model design have many revolute joints between wheels and the body. The number of revolute joints

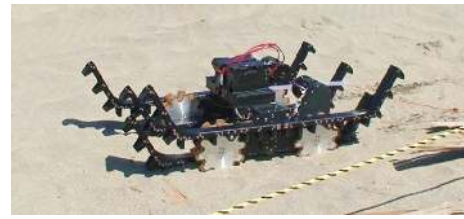


Fig. 4. Prior "Crank-Wheel" having 2 pairs of crank legs and inverse U-shaped body.

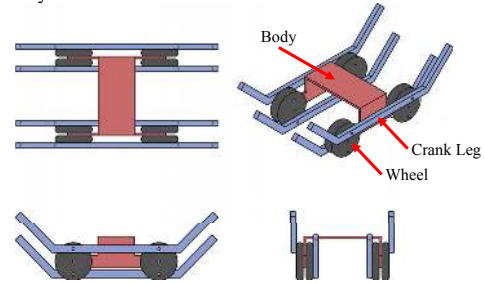


Fig. 5. Schematic illustration of prior Crank-Wheel. The crank legs, the body, and the wheels are indicated in blue, red, and green, respectively.

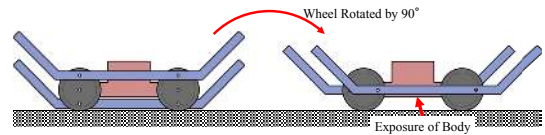


Fig. 6. Image of Crank-Wheel when the wheels are rotated by 90 degrees. Crank legs are at the same height and the body, which has no grouser, is exposed. If the edge of the obstacle enters the gap between the wheels, the body will make contact with the obstacle, thereby causing slippage.

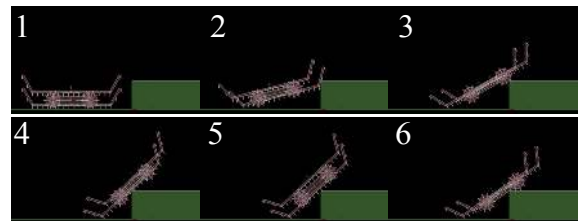


Fig. 7. Physics simulation result of step climbing with the model whose parameters are same as that of the Crank-Wheel model. If the friction coefficient is not sufficiently high, the body slips and falls off, and the model cannot climb the step.

in the prior Crank-Wheel model is 8, while that of the simple model is only 4.

Another problem faced by this model is the exposure of the smooth surface of the body. When viewed from the side, the body is exposed at a particular wheel phase (Fig.6). In this vehicle, the crank legs do not slip easily because of the attached grousers. However, the under-side of the body is flat shaped and does not have a grouser. Therefore, the vehicle may slip when it comes in contact with protrusions like the edges of stairs. Fig.7 shows the results of the physics simulation[10] for step climbing. In this simulation, the physics model of Crank-Wheel has almost the same shape as that of the hardware prototype; it has 2 crank legs in the z-x plane, because the Crank-Wheel has 2 pairs of crank legs. In an environment where the friction coefficient was set to 0.5, the body slipped when the wheel phase was similar to

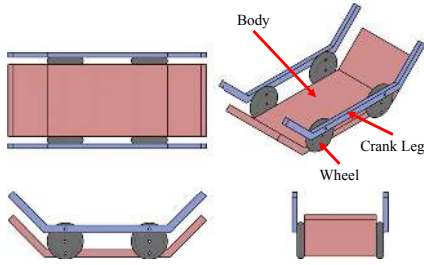


Fig. 8. Schematic illustration of Eccentric Crank Rover. The body part also acts as a second crank leg.

that shown in Fig.6, and could not climb the steps.

To summarize this section, the problems faced by prior models are as follows.

- Simple Model
 - Oscillation of necessary torque.
 - Clearance height from front.
- Crank-Wheel
 - Complicated body.
 - Exposure of smooth surface.

III. CONCEPT

In this research, we solve these problems using our proposed "Eccentric Crank Rover"(ECR). Fig.8 is a schematic illustration of the ECR. As shown in the figure, the ECR has only 1 pair of crank legs, and four wheels are attached to the driving shafts in eccentric positions. In this concept, the offset radius of the joint of crank leg and the driving shaft from wheel center is same; however, they are in 180° opposite position.

A. Function of the Body as a "Second" Crank Leg

The structure of the body is simple and the number of revolute joints between the wheels and the body is 4, which is similar to that of the simple model. In addition, the ECR addresses the problem of slippage on smooth surfaces by attaching grousers to not only the crank legs but also the body. At the same time, the shape of the body in the side view is identical to the crank legs.

Furthermore, the trajectory of the body follows the same trochoid curve as the crank legs, but in an opposite phase, as shown in Fig.9. This is because the eccentric radius of the body and the crank legs is identical, while the phase difference is 180 degrees. Namely, the body effectively acts as the "second" crank leg, and moves alternately with the crank legs.

To confirm the feasibility of this concept, the physics simulation experiment, as shown in Fig.10, was performed. The vehicle model in this simulation was basically same as that in the former simulation (Fig.7), with the exception being that the body part of the former model was removed, and 1 pair of crank legs was regarded as the body, in order to replicate the structure of the ECR. As shown in the figure, the ECR model successfully climbed the step without slippage.

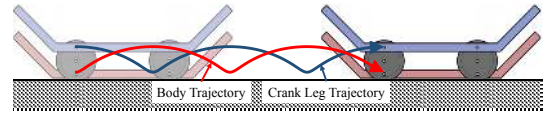


Fig. 9. Trajectory of the body and the crank legs. The body moves along same trajectory because of the eccentric wheel.

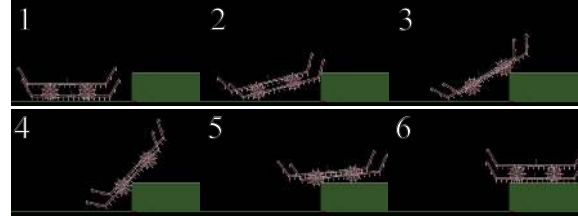


Fig. 10. Result of physics simulation for step climbing with the model, wherein the body is removed from the model in Fig.7.

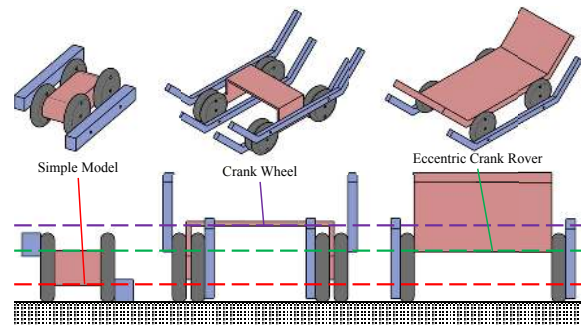


Fig. 11. Comparison of the 3 models from the front view. The ECR attains a relatively large clearance height despite its structural simplicity.

B. High Clearance under the Body

Fig.11 shows the comparison between the simple crank wheel model, the prior Crank-Wheel model, and the ECR model in front view. The wheel diameters of all models are identical. Each dotted line indicates the maximum bottom line of each model. The ECR is in the position where the body attains the maximum height. The prior Crank-Wheel model has highest ground clearance because of its inverse U-shape body. In contrast, the ECR has relatively high clearance despite its quite simple structure. This implies that the ECR makes it difficult for the vehicle to be obstructed by protrusions because of the eccentric wheel.

C. Statically Balanced Running

The effectiveness of the eccentric wheel is not only in terms of rough terrain mobility, but also in terms of energy efficiency. While running on flat ground, the mechanism incorporating the oscillation of necessary torque or potential energy has less energy efficiency than the mechanism wherein no such oscillations are present, because the oscillation of torque or potential energy results in the generation of negative work or driving actuators in an inefficient area. In the ECR mechanism, such oscillations caused by crank legs are cancelled out by the eccentric wheel and mass arrangement.

Fig.12 shows the schematic illustration of the ECR. In this analysis, both crank legs are in the same phase, and can be

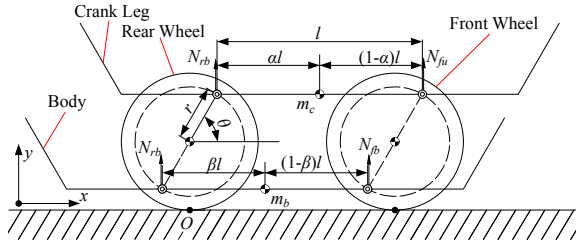


Fig. 12. Schematic image of ECR in the side view. If the mass of body and total mass of 1 pair of crank legs are the same, the moment generated on each wheel by the weight of body and crank legs becomes zero, and the static balance of this system is maintained for all θ .

considered as one linkage. m_c is total mass of 1 pair of crank legs, and m_b is the mass of the body. $N_{fu}, N_{fb}, N_{ru}, N_{rb}$ are the vertical forces that the crank legs and the body receive from wheels in each position. These forces can be calculated from balance of moment, as follows.

$$\begin{cases} N_{fu} = m_c g \alpha \\ N_{fb} = m_b g \beta \\ N_{ru} = m_c g (1 - \alpha) \\ N_{rb} = m_b g (1 - \beta) \end{cases} \quad (1)$$

The moment on each wheel applied by these forces can be represented as follows.

$$\begin{cases} M_F = (-N_{fu} + N_{fb})r \cos \theta \\ = (-m_c \alpha + m_b \beta)gr \cos \theta \\ M_R = (-N_{ru} + N_{rb})r \cos \theta \\ = (-m_c (1 - \alpha) + m_b (1 - \beta))gr \cos \theta \end{cases} \quad (2)$$

Where M_F is the total moment of the front wheel, and M_R is the total moment of the rear wheel. The wheels, the body, and the crank legs comprise the parallel link; thus, both the front and rear wheels always are synchronized and their phase, θ , become identical. Thus, the torque loaded to each wheel is transmitted to the other wheel. Then summation of the torque loaded to both wheels can be represented as follows.

$$M_F + M_R = (-m_c + m_b)gr \cos \theta \quad (3)$$

Therefore, the moment loaded to wheels by gravity becomes zero regardless of the wheel phase, if the mass of the body and the total mass of 1 pair of crank legs are the same. Therefore, it is possible to achieve a statically balanced running vehicle using this concept of the ECR, if the mass of the body and crank legs are accordingly adjusted.

IV. DESIGN

Based on the above mentioned concepts, the hardware prototype of the ECR mechanism was designed. Fig.13 shows the illustrations of the ECR, and Table I is the specifications of ECR. To achieve weight balancing mentioned in Section Section III-C, batteries are affixed on each side of crank legs, during the installation of the motors in the body. In order to adjust weight balancing, about 60 g of additional weight was attached to each crank leg.

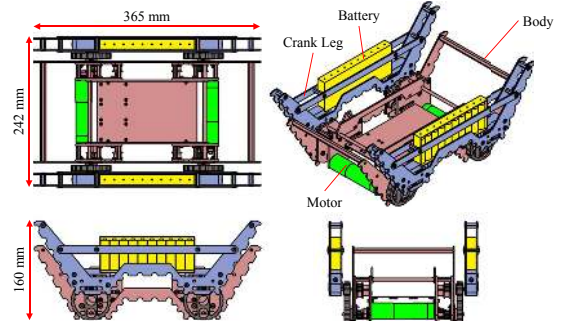


Fig. 13. Illustration of ECR. Similar to the former schematic images, the body is indicated in red and the crank legs are indicated in blue. Furthermore, the motors in green, and the batteries are indicated in yellow. All the batteries are located in the crank legs in order to achieve static balance of the body and the crank legs.

TABLE I
SPECIFICATION OF ECR

Length	365 mm	Total Weight	2809 g
Width	242 mm	Body Weight	1363 g
Height	160 mm	Crank Weight (1 Pair)	1363 g
Wheel Diameter	64 mm	Wheel Weight (Total)	83 g
Number of DOFs	2		

A. Geometrical Design

The shape of crank legs, wheels, and grousers are determined heuristically using physics simulation, as shown in Fig.14. After adopting several trial configurations, the mechanism successfully climbed the 150 mm step in the physics simulation. An innovative feature of this design is the concaves of the bottom surface of the crank leg and the body. These concaves reduce the pitching angle when climbing a high step, and prevent the body from standing vertically.

Fig.15 illustrates the schematic of the wheel designed for ECR. In order to make comparative experiments, this wheel is attached to different points of the drive shaft not only in eccentric position, but also at the center position. The other hole opened in eccentric position is for bearings of the crank legs.

B. Control System

Fig.16 is schematic illustration of the electrical system of ECR. The power source comprises 20 cells of AA size Ni-H battery. Two sets of 10 cells each are mounted in each crank leg. All the cells are connected in series, resulting in a total voltage of 24 V. The motor drivers are "1-axis DC Power Module" (Hibot Corp.), and a microcomputer board is "TITech M4 Robot Controller" (Hibot Corp.), and 5 V DC-DC converter is used for this board. Commands are input using the gamepad, and received by the bluetooth module, "SBRCB3BT" (Running Electronics). The motors used are RE25 DC motors (maxon motor).

V. EXPERIMENT

In this study, the step climbing experiment, the protrusion traversing experiment, and the flat plane running experiment were performed. The developed ECR can construct 4 types of vehicle structures, as shown in Fig.17, because of the

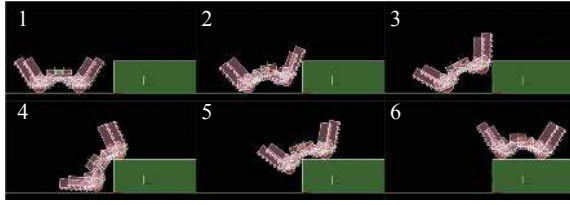


Fig. 14. Physics simulation of ECR with heuristic parameters. The parameters obtained from this simulation was also used in the hardware prototype of ECR.

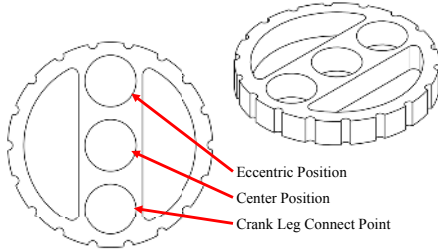


Fig. 15. Wheels developed for ECR. This wheel possesses 3 holes: one to attach bearings of crank legs, another to connect the drive shaft in the center position, and the third to connect the drive shaft in eccentric position.

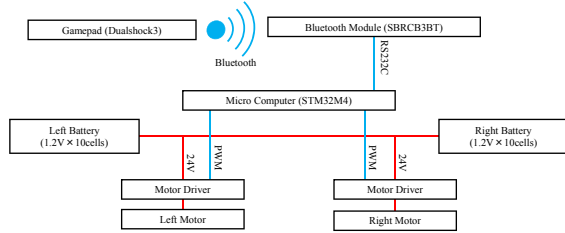


Fig. 16. System of ECR. Red lines are the electric power, and blue lines are the communication line.

multi-holed wheel design mentioned in section IV-A. As shown in this figure, "normal model" is a vehicle without both crank legs and eccentric wheels, "eccentric model" is a vehicle with only eccentric wheels, "crank model" is a vehicle with only crank legs, and "ECR model" is a vehicle which is equipped with both crank legs and eccentric wheels. The normal model is a model of normal wheel mechanism. Eccentric model is an effective model that addresses the problem of clearance under the body, mentioned in Section II-A and III-B because the bottom height of the body rises, similar to the ECR model. The crank model addresses the body slippage problems mentioned in Section II-B and III-A because the body of the crank model is equipped with grousers.

A. Climbing Step

Fig.18 shows an experiment involving step climbing. In this experiment, various heights of steps are experimented with, and the height climbed by each model is measured. The results of this experiment are shown in Fig.19. As a result, the eccentric model and ECR model have higher climbable step height than other non-crank leg models because the grousers of crank legs and body grasp the edge of the step alternately, as that in a walking mechanism. Further, the ECR model achieved the climb using a smaller number of rotations than

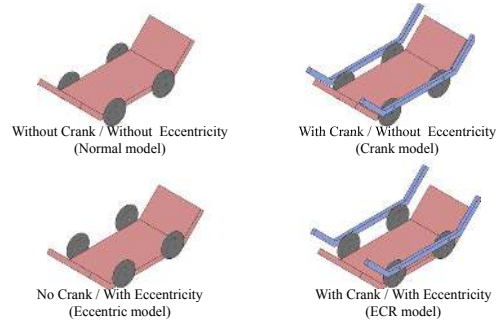


Fig. 17. Schematic illustrations of vehicle models experimented in this study. There are 4 models depending on whether the vehicle is equipped with crank legs or not, and whether the vehicle possesses eccentric wheels or normal wheels.

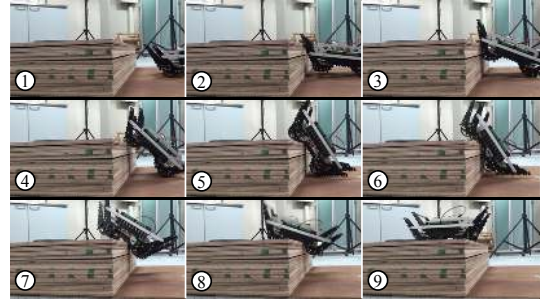


Fig. 18. Step climbing experiment with a 150 mm step using the ECR model. This model successfully climbed the same height step similar to the physics simulation in Fig.14.

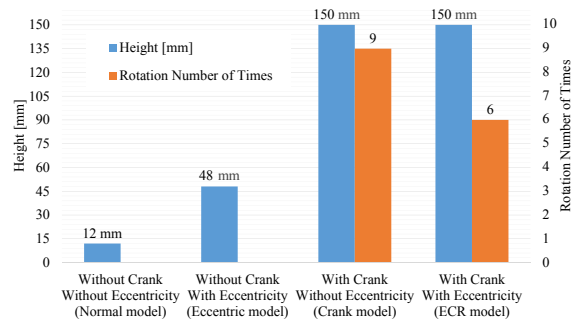


Fig. 19. Result of step climbing experiment with 4 vehicle models. The blue bars indicate the maximum step height each model could climb, and orange bars indicate the number of rotations required for climbing the steps.

the eccentric model. Thus, ECR model could climb faster than the eccentric model, because the stride of body and crank legs are larger.

B. Traversing Protrusion

Fig.20 and Fig.21 show the protrusion traversing experiment with crank model and ECR model. In both cases, the height and width of protrusions were 36 mm. The crank model could not traverse across the protrusion because its body interfered with the protrusion; however, the ECR model traversed successfully because of the large clearance height. Identical to these results, the normal model could not traverse, while the eccentric model traversed successfully.



Fig. 20. Protrusion traversing experiment with crank model. This model could not successfully traverse the protrusion because its clearance height was lower than the protrusion; consequently, the body interfered with the protrusion.

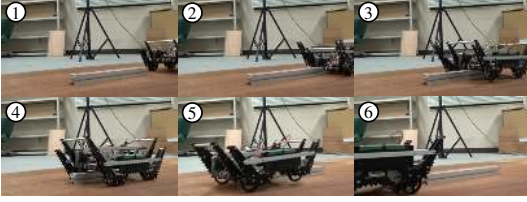


Fig. 21. Protrusion traversing experiment with ECR model. This model successfully traversed the protrusion because its maximum clearance height was higher than the protrusion.

C. Energy Efficiency on Flat Ground

The current consumptions of each model when running on flat ground were measured. Fig.22 shows the results of this measurement experiment. This data was measured when the models were at a constant speed of 0.37 m/s. In order to ensure the mass of each model were identical, the crank legs were mounted on the body of the normal model and the eccentric model.

As shown in the graph, the current consumptions of the eccentric model and crank model have oscillation in one cycle. In contrast, those of the normal model and ECR model are almost constant. Based on this result, the cost of transport (COT) of the 4 models were calculated, as shown in Fig.23. Therefore, the eccentric model, which is lifting up own weight in every cycle had the worst COT, and crank model which rise up the weight of crank legs in every cycle was second the worst. The normal model and ECR model, which are always statically balanced, have almost identical values of COT. Therefore, the energy efficiency of the ECR mechanism is almost the same as that of the normal wheel vehicle.

VI. CONCLUSIONS

In this study, in order to address the drawbacks of prior models, we proposed a novel crank wheel mechanism, "Eccentric Crank Rover", which has eccentric wheels for mobility and efficiency, and described its effectiveness in terms of rough terrain mobility and energy efficiency. The ECR mechanism was developed, and comparative experiments were conducted to confirm its step climbing ability, anti-stuck ability, and energy efficiency. The major issue with the ECR, at present, is the low integrity of the robot. The present model is ill equipped to traverse dirty environments, such as lack of waterproofing or dust-proofing, which is absolutely necessary for its application as a rough terrain vehicle. We believe that the ECR mechanism can achieve a low COT identical to other wheel vehicles; moreover, robustness against dirty environment can be realized by polishing its hardware and software.

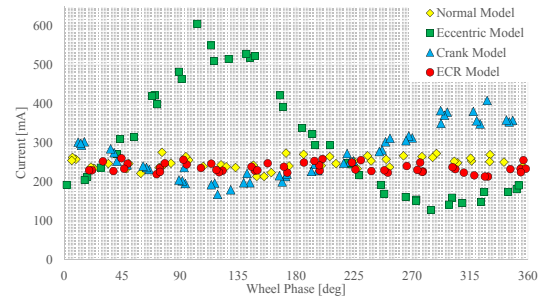


Fig. 22. The results of current measurement of running on flat ground for all 4 vehicle models. The abscissa is the current in motor, and the ordinate is the wheel phase. In each model, the origin of wheel phase is the point where the body is at lowest position and crank legs are at highest position. This measurement was carried out for more than 8 rounds of wheels.

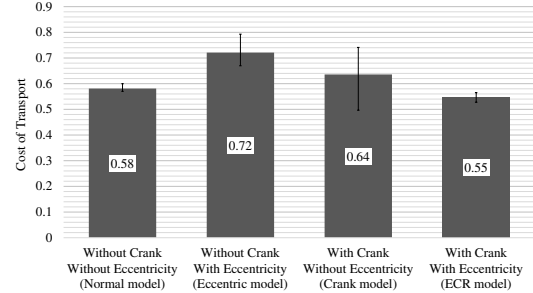


Fig. 23. Cost of transport for each model. The energy consumption was calculated from the average of left and right current, as shown in Fig.22. These values do not include hotel load.

VII. ACKNOWLEDGMENT

This work was supported in part by Program for Leading Graduate Schools "Academy for Co-creative Education of Environment and Energy Science", MEXT, Japan.

REFERENCES

- [1] M. Arai, Y. Tanaka, and S. Hirose, "Development of "souryu-iv" and "souryu-v:" serially connected crawler vehicles for in-rubble searching operation," *Journal of Field Robotics*, vol. 31, no. 65, pp. 31–65, 2008.
- [2] B. Yamauchi, "Packbot: A versatile platform for military robotics," in *Proceedings of SPIE 5422*, 2004, pp. 228–237.
- [3] M. Raibert, "BigDog, the Rough-Terrain Quadruped Robot," in *Proceedings of the 17th IFAC World Congress, 2008*, M. J. Chung, Ed., vol. 17, no. 1.
- [4] H. Komura, H. Yamada, and S. Hirose, "Development of snake-like robot acm-r8 with large and mono-tread wheel," *Advanced Robotics*, vol. 29, no. 17, pp. 1081–1094, 2015.
- [5] H. Komura, H. Yamada, S. Hirose, G. Endo, and K. Suzumori, "Study of swing-grouser wheel: A wheel for climbing high steps, even in low friction environment," in *Intelligent Robots and Systems (IROS), 2015 IEEE/RSJ International Conference on*, Sept 2015, pp. 4159–4164.
- [6] M. W. Thring, *Robots and telechairs : manipulators with memory, remote manipulators, machine limbs for the handicapped*. Ellis Horwood, 1983.
- [7] K. C. Galloway, G. C. Haynes, B. D. Ilhan, A. M. Johnson, R. Knopf, G. Lynch, B. Plotnick, M. White, and D. E. Koditschek, "X-rhex: A highly mobile hexapedal robot for sensorimotor tasks," University of Pennsylvania, Tech. Rep., 2010.
- [8] G. Gabrielli and T. H. von Karman, "What price speed?" in *Mechanical Engineering*, vol. 72, no. 10, 1950, pp. 775–781.
- [9] H. Nakano and S. Hirose, "Crank-wheel: A brand new mobile base for field robots," in *IROS*. IEEE, 2012, pp. 4608–4613.
- [10] "Box2d a 2d physics engine for games," <http://box2d.org/>.